Graphene oxide-branched polyethylenimine foams for efficient removal of toxic cations from water

Dawid Pakulski, [abc] Włodzimierz Czepa,[abc] Samanta Witomska,[abc] Alessandro Aliprandi,[a] Piotr Pawluć,[c] Violetta Patroniak,*[b] Artur Ciesielski*[a] and Paolo Samorì*[a]

[a] *Université de Strasbourg, CNRS, ISIS, 8 alleé Gaspard Monge, 67000 Strasbourg, France, E-mail: ciesielski@unistra.fr; samori@unistra.fr*

[b] *Faculty of Chemistry, Adam Mickiewicz University, Umultowska 89b, 61614 Poznań, Poland, E-mail: violapat@amu.edu.pl*

[c] *Centre for Advanced Technologies, Adam Mickiewicz University, Umultowska 89c, 61614 Poznań, Poland*

† Electronic Supplementary Information (ESI) available. See DOI:10.1039/x0xx00000x

Highly porous foams based on graphene oxide functionalized with polyethylenimine are generated and used with unprecedented efficiency for adsorbing heavy metal ions. A multiscale analysis of the GO-BPEI nanocomposite provided evidence for the covalent grafting of BPEI on GO and the formation of low crystalline porous foams. The uptake experiments revealed that the GO-BPEI's adsorption of toxic cations is strongly dependent on the pH in range from 2 to 10, as a result of the different interactions at the supramolecular level between the metal ions and the GO-BPEI foam. The maximum uptake capacities for Cu(II), Cd(II) and Pb(II) are achieved at pH = 5 and exhibit values as high as 1096, 2051 and 3390 mg g^{-1}, respectively, being ca. over 20 times greater than standard sorbents like activated carbon. The GO-BPEI composite can be easly regenerated as proven by performing adsorption cycles. Also, the thermodynamic parameters including standard Gibbs free energy (ΔG^o), the enthalpy change (ΔH^o) and entropy change (ΔS^o) revealed the exothermic and spontaneous nature of the adsorption process.

The rapid escalation of agricultural and industrial activities as a result of the population growth is yielding a dramatic increase of the number of pollutants released worldwide on a daily basis into the environment. These contaminants, which are very diverse in nature and range from heavy metals and distillates to micropollutants such as nitrosamines[1] and endocrine disruptors,[2] represent one of the largest public health and environmental concerns.[3, 4] As a consequence, there is a need for developing new robust technologies for low-cost and effective removal of contaminants from water.[5] Among them, adsorption processes, based on the capturing of the pollutant (i.e. analyte) by an adsorbent (i.e. receptor) is a chemically programmable approach, which relies on supramolecular recognition events. The development of *ad hoc* receptors makes it possible to exploit this extremely versatile strategy in a variety of environments.[6-9] Moreover, by taking advantage of the reversible nature of non-covalent interactions, the regeneration of the adsorbent enables its use multiple times. Typically, hygroscopic materials such as activated carbon (AC)[10] are being exploited as adsorbent due to their remarkable capacity to adsorb a wide range of pollutants.[11] Nevertheless, the wide use of activated carbon is hampered by its processing and high production cost, limited chemical selectivity and the severe regeneration processes.[12] Alternative adsorbents based on nanoparticles[13] metal organic frameworks (MOF)[14] and carbonaceous materials such as carbon nanotubes (CNTs) and graphene have been proposed.[15-18] Compared to CNTs, the use of two-dimensional materials (2DMs) as platforms for development of new adsorbents offers various advantages. 2DMs are atomically thick and

possess two planar surfaces available for contaminant adsorption, thus featuring extremely high surface-to-volume ratio. Moreover, graphene can be easily produced in the form of graphene oxide (GO) which displays numerous oxygen-rich functional groups such as carbonyls, epoxides, and hydroxides that act both as reactive sites for further covalent functionalizations[19-22] and can interact *via* dipole-dipole or strong electrostatic interactions with the pollutant molecules, enhancing the occurrence of adsorption events. By mastering such interaction types, a variety of GO-based systems have been designed[23] as adsorbents for the removal of inorganic species from aqueous solutions.[24-26] Noteworthy, because of its chemical nature GO is highly hydrophilic and its exposure to humid environment results in weight increase.[27] Interestingly, the hydrophilic nature of GO can be enhanced through the introduction of nitrogen atoms *via* chemical reactions.[28] By taking also advantage of GO's ability to assemble into highly porous structures, its capacity to adsorb cations is much greater than any other known sorbent.[29, 30] In particular, it was shown that neat GO has a high absorption capacity for Cu(II) (223 mg g^{-1}), Cd(II) (530 mg g^{-1}), and Pb(II) ions (1120 mg g^{-1}).[31] Numerous factors, such as pH and ionic strength have been found to influence the adsorption capability of metal ions on GO. In particular, the pH_{pzc} (point of zero charge) value of GO was estimated as 3.9,[32] and therefore the surface of GO is positively charged at pH < pH_{pzc}, and is negatively charged at pH > pH_{pzc}. Such behavior can be ascribed to the protonation of hydroxyl and carboxyl moieties, making GO positively charged thereby leading to the emergence of repulsive interactions with the metal cations.[33, 34]

Overall, extensive efforts have been devoted towards the development of GO-based adsorbents (GOAs) through the GO functionalization with both inorganic and organic molecules; yet, several obstacles must be overcome to enable their use in daily-life. A major limitation is that most of the existing GOAs are water soluble, and therefore they cannot be easily removed and regenerated after adsorption of pollutants. In order to solve this issue, bridging of GO layers using molecular pillars to form three-dimensional (3D) macroscopic porous structures is an essential step to tailor GOAs properties, simultaneously by preserving many of the unique properties of the individual GO sheets and by benefitting from the presence of molecular linkers. Such approach is being pursued and experimental results showed that 3D GO-based materials possess porous structures and high specific surface areas,[35-37] making them ideal for applications as adsorbent of heavy metal ions. In this context, the fabrication of 3D GOAs through covalent linkage between individual GO sheets is extremely appealing, as it could result in a remarkable enhancement of the adsorption capacity.

In the past few years, GO/branched polyethylenimine (GO-BPEI) hybrid structures generated through the condensation of the carbonyl moieties and ring-opening reactions of the epoxy groups (Figure 1), was applied as composite for numerous applications including humidity sensing,[38] adsorption of organic dyes and gasses,[36] energy storage [39] and biochemical,[40-42] to name a few. BPEI itself has been widely used for encapsulation or adsorption of guest molecules.[43] In particular, branched polyethylenimine is a biocompatible compound and, as a result of its chemical structure, it has strong capacity to interact at the supramolecular level with heavy metal ions.[44, 45] BPEI in fact incorporates a high number of amine groups, which exist in primary, secondary and tertiary forms,[46, 37] with a branching site at every 3-3.5 nitrogen atom in any given BPEI chain segment, which can be potentially protonated. Thus, at low pH of the solutions BPEI has a high cationic charge density, therefore it can form coordination complexes with heavy metal ions solely in environment characterized by a pH close to neutral or in basic solutions.[47]

Here we describe a facile approach to the *bottom-up* fabrication of 3D GO-based adsorbent. The adsorption kinetics and isotherms of Cu(II), Cd(II) and Pb(II) ions on GO-BPEI hybrid at various pH are estimated with the pseudo-first and -second order as well as Freundlich and Langmuir isotherm models. In particular, we show that the adsorption capacity of GO-BPEI foam prepared *via* condensation reaction is much higher than the one of any known sorbent including neat or functionalized GO. Moreover, we show that the GO-BPEI foam saturated with metal ions can be regenerated upon treatment with either ethylenediaminetetraacetic (EDTA) or nitric acid. The presented results demonstrate the great potential of GO-based composites in wastewater purification and represent a notable step forward in the effort of removing toxic metal pollutants from water at a large scale.

Cross-linking between GO and BPEI has been previously reported.[36, 39, 42] BPEI solution in ethanol is added into suspension of GO in water/ethanol mixture 1:1 *vol:vol* and rigorously stirred overnight under reflux (see *Experimental Section* for details in ESI†). Unreacted BPEI molecules are washed away and resulting GO-BPEI is then freeze-dried for 48 h under vacuum. To get a morphological insight, scanning electron microscopy (SEM) images are recorded. Figure 2a portrays the homogeneous porous structure of GO-BPEI foam. Furthermore, energy-dispersive X-ray spectroscopy (EDX) analysis (Figure 2b) shows the uniform distribution of the BPEI component within the GO-BPEI foam.

Fourier transform infrared spectroscopy (FTIR) spectra of GO, BPEI and GO-BPEI are shown on Fig. S1, ESI†. The spectrum of GO displays its well-known features, i.e., C=O stretching at 1731 cm^{-1}, C=C stretching at 1620 cm^{-1}, C-O stretching of epoxy groups at 1047 cm^{-1}. Typically, cross-linking reaction between GO and BPEI results in the formation of amides (at the edges of GO flakes) and opening the epoxy groups (located on the plane of the of GO flakes).[37] Indeed, after the reaction with BPEI, small shift of C=O groups (1590 cm^{-1}) is monitored and assigned to the formation of amide bonds resulting from the condensation between carboxylic groups of GO and primary amines of BPEI. Noteworthy, while opening of GO's epoxy groups determines the disappearance/shift of the band at 1047 cm^{-1}, because of the presence of C-N bonds, which originate from BPEI component, the spectra of GO-BPEI exhibit a notable signal at 1040 cm^{-1}. The formation of the GO-BPEI composite is further evidenced by the appearance of C(aliphatic)-H signals at ca. 2900 cm^{-1} which is not present in the neat GO.

The GO-BPEI was further characterized by Raman spectroscopy a non-destructive technique used to study the structural changes of graphene oxide based materials. In general, chemical modification of graphene-derived materials is often characterized by the changes in the ratio of the D and G bands. After the functionalization of GO with BPEI the I_D/I_G intensity ratio increases from 1.00 to 1.30, and is attributed to the increase of the sp^3 carbon atoms after functionalization, and is consistent with other reports (see part *Raman analysis* and Figure S2 in ESI†).

The cristallinity, and in particular the interlayer distance (d_{002}) between functionalized GO sheets within GO-BPEI foam, is characterized by wide-angle X-ray scattering (WAXS). The starting material, i.e. GO, displays a typical sharp peak at 10.02° corresponding to an interlayer spacing of 0.88 nm due to the (002) reflection of stacked GO sheets (Figure S3, ESI†), in line with the values reported previously.[48, 49] The 2θ peak of the as-prepared GO-BPEI foam disperses in wide range of angles (7°-16.30°) highlighting nonhomogeneous nature of the foam-like composite, and indicates large changes in the crystalline nature if compared with GO. Based on the Bragg equation, the d_{002} spacing is calculated in a range from 0.54 to 1.23 nm and it is ascribed to alternation of GO interlayer spacing[50] as a result of the functionalization with BPEI and partial reduction of GO, which typically occurs in ethanol upon

thermal annealing.[51, 52] The wide range of dispersion angle is caused by nonhomogeneous structure of product.

X-ray photoelectron spectroscopy (XPS) is exploited to unravel the chemical composition of hybrid material by identifying the relevant chemical elements present in both GO and GO-BPEI. This method is also applied to study the chemical nature of metal ions adsorbed on GO-BPEI. The significant difference between the carbon, oxygen and nitrogen peaks provided the evidence on the chemical bond formation between the oxygen-containing functional groups on the surface of GO and amine groups from BPEI. (see *XPS analysis* for details in ESI†)

The thermal stability of GO, BPEI and GO-BPEI are investigated using thermal gravimetric analysis (TGA). The GO curve displays a weight loss of ca. 50% in range of 150-300 °C caused by decomposition of oxygen functional groups.[53] Conversely, GO-BPEI undergoes degradation in two steps. At first over 100° C the deoxygenation process is observed which determines ca. ~10% weight loss. Sharper drop of mass percentage is monitored around 300 °C and it can be associated to the BPEI's thermal degradation (see Fig. S7, ESI†).[54]

The porosity of GO-BPEI is characterized by N_2 adsorption–desorption isotherms measurement at 77 K. The starting material of GO displays a specific surface area of ca. 10 m^2 g^{-1}. Depending on the level of water content, the specific surface area of GO calculated with Brunauer-Emmett-Teller (BET) model falls in the range from 10 to 100 m^2 g^{-1}. The average pore diameter calculated with the Barrett-Joyner-Halenda (BJH) model amounts to 13.1 nm (Fig. S8 in ESI†). A specific surface area of GO-BPEI is calculated as 220 m^2 g^{-1}. Compared to GO, the notable increase of the specific surface area of the GO-BPEI indicates that the interlayer cross-linking BPEI acts as spacer, thereby hindering the stacking between adjacent GO layers, leading to notably greater accessible surface area for the adsorption of N_2 (see Fig. S9 and Table S1, ESI†).

The uptake of the metal ions is then carried out by the means of the adsorption experiments by mixing GO-BPEI and Pb(II), Cd(II) and Cu(II) aqueous solutions at the desired concentration and pH. For the sake of comparison, control experiments, in which neat compounds of GO or BPEI are used as adsorbents, are also carried out (see *Experimental Section* for details in ESI†). The pH of the solutions of salts are adjusted with HNO_3 (0.1 M) and KOH (0.1 M) and filtered through polytetrafluoroethylene (PTFE) membranes (0.22 µm). Subsequently, GO-BPEI foam is added into the salt solution and pH is re-adjusted. Because of the highly hygroscopic nature of carbon-based adsorbents (e.g. activated carbon), the uptake performance cannot be assessed by the means of gravimetric analyses, since the mass of porous carbon-based materials may vary as a function of humidity. Therefore, spectroscopic techniques have to be employed. In particular, the concentration of metal ions remaining in the solution is determined by using flame atomic absorption spectrometry (F-AAS). In particular, the amount of metal ions captured by GO-BPEI (mg g^{-1}) is calculated from the difference between the initial (C_0; mg L^{-1}) and the equilibrium (C_e; mg L^{-1}) concentration by using applying Equation 1, where V is the volume of the metal ion solution, and $m_{adsorbent}$ is the mass of GO-BPEI.

$$q_e = \frac{(C_0 - C_e) \times V}{m_{adsorbent}} \qquad \text{(Equation 1)}$$

The adsorption isotherms for GO-BPEI as well as for the control samples are fitted better by the Langmuir model than by the Freundlich model (see Figure 3 and Table S2-3 in ESI†), suggesting that sorption of metal ions onto GO, BPEI and GO-BPEI foam is not exciding monolayer coverage. The maximum adsorption capacity (q_{max}) values of Cu(II), Cd(II) and Pb(II) on GO-BPEI (see Table S2, ESI†) are 1096, 2051, and 3390 mg g^{-1}, respectively. The q_{max} values

expressed in mmol g^{-1} amount to 17.3 ± 0.4, 18.3 ± 0.5 and 16.4 ± 0.4, and, for Cu(II), Cd(II) and Pb(II), respectively, implying that 1 g of GO-BPEI foam can adsorb ca. 17 mmol of divalent metal ions from 1 L of contaminated water. The results of adsorption experiments of heavy metal ions on GO-BPEI are benchmarked with activated carbon (AC) and AC modified with polyethyleneimine (AC-PEI). The experimental results discussed in the ESI† (see Figures S10-11, and Tables S4 ESI†) reveals that GO-BPEI outperforms AC. In particular, the q_{max} values of Cu(II), Cd(II) and Pb(II) sorption on AC are 0.88 ± 0.03, 0.77 ± 0.02, and 0.68 ± 0.02 mmol g^{-1}, respectively. As reported in the literature, the q_{max} values for AC chemically modified with polyethyleneimine (AC-PEI) amount to 0.40, 0.26 and 0.13 mmol g^{-1} for Cu^{2+}, Pb^{2+} and Cd^{2+}, respectively,[55, 56] being ca. over 40, 60 and 160 times lower than GO-BPEI. A comparison of q_{max} values with those previously reported for chemically modified graphene have been presented in Tables S5-7 in ESI†.

The absorption behavior of the metal ions GO-BPEI foam as a function of time is portrayed in Figure S13, ESI†. It reveals that the adsorption displays a remarkable increase at the beginning of the experiments and then it reaches a plateau. The time required to reach such equilibrium state depends on metal ions. Unlike in the case of unfunctionalized GO, where the metals adsorbs rapidly (plateau reached after ca. 20 min) on its surface,[31] the adsorption equilibriums for GO-BPEI are obtained only after 300 min, 350 min and 400 min for Cu(II), Cd(II) and Pb(II), respectively (see *Kinetic study* for details in ESI†). The adsorption of metal ions on the GO-BPEI foam is then investigated at pH values ranging from 2 to 10. Noteworthy, the pH of solution plays a crucial role in the adsorption of metal ions. The thermodynamic analysis (see Fig. S14 and Table S10 in ESI†) of the adsorption of heavy metal ions on GO-BPEI at various temperatures revealed the exothermic nature of the process. The negative values of ΔGº at various temperatures indicated the spontaneous nature of the adsorption process, which was further confirmed by ΔH° analysis. The positive values of ΔSº suggest that conformational changes occur in GO-BPEI foam during the adsorption process. This might be also attributed to the substitution of water hydration molecules by metal ions in the coordination pockets.

In particular, while the Cd^{2+} remain as dominant specie in a wide range of pH, at pH values from 6 to 10 Pb^{2+} and Cu^{2+} are replaced by $PbOH^{+}$ and $CuOH^{+}$, respectively.[31] As shown in Figure 4, in the case of control experiments the maximum adsorption of metal ions on GO (Fig. 4a) and BPEI (Fig. 4b) is reached at pH 4 and 5, respectively. The adsorption experiment on GO-BPEI foam shows similar results and q_{max} for all metal ions is reached at pH 5 (Fig. 4c). The uptake capability of heavy metal ions by GO-BPEI increases significantly at pH 5, reaching its maximum, then slowly decreasing at higher pH values. At low pH values ($pH < pH_{pzc}$), the surface of GO-BPEI foam is positively charged, and the adsorption of heavy metal ions is in competition with protonation of the nitrogen containing anchoring groups of the BPEI fragment. As a result, segments of BPEI polymer, which serve as supramolecular pockets at neutral pH becomes unable to coordinate the metallic species. Conversely, an increase in the pH ($pH > pH_{pzc}$) leads to neutralization of the positive charges on the foam surfaces, which result in an increased capacity to adsorb metal ions. Nonetheless, as aforementioned, the adsorption of metal ions at high pH values is mainly affected by the type of dominant form they adopt in the solution. In particular, at high pH our ions exist as $PbOH^{+}$ and $CuOH^{+}$ thus their non-covalent interactions, i.e. electrostatic and coordination bonds, with GO-BPEI composite is evidently weakened. The difference in the affinity of metal ions to the GO-BPEI foam is then studied by the means of uptake experiments using binary and ternary mixtures. Towards this end, the competitive adsorption of binary and ternary aqueous solutions in mixtures Pb(II)/Cu(II), Pb(II)/Cd(II), Cu(II)/Cd(II), and Pb(II)/Cu(II)/Cd(II) on the GO-BPEI is

explored using fixed amount of each metal ions, i.e. 17 mM per 1 g of GO-BPEI, being the maximum loading of GO-BPEI foam for single metal cations at pH = 5 (see Figure S15, ESI†). Noteworthy, the adsorption of Cd(II) on GO-BPEI decreased sharply in the presence of Pb(II) and Cu(II). Because the affinities of Pb(II) and Cu(II) to GO-BPEI foam are stronger than that of Cd(II), the former ions are adsorbed preferentially, which leads to the lower uptake of Cd(II). Remarkably, the affinity of Pb(II) and Cu(II) ions is nearly identical, as evidenced by the results of Pb(II)/Cu(II) uptake experiments. Moreover, the results of ternary mixture uptake further confirm the affinities observed for binary mixtures and reveals that the affinity of GO-BPEI foam for the three metal ions follow the order of Pb(II) ≈ Cu(II) >> Cd(II). This order slightly differs from that of neat components. The affinity of unfunctionalized GO towards heavy metal ions has been experimentally defined as Pb(II) >> Cu(II) >> Cd(II), therefore it directly reflects the strength of non-covalent (electrostatic) interactions, which decreases as a function of electronegativity and stability constant of the associated metal hydroxides.[31] As the adsorption of metal cations occurs on a negatively charged surface, the attraction for negative charges plays a significant role in the adsorption process. Therefore, both electronegativity of metal ions and the stability constants can be considered as contributing parameters. The affinity of neat GO towards heavy metal ions agrees very well with stability constant of the associated metal hydroxides ($Me^{2+} + OH^- \leftrightarrow Me(OH)^+$; $\log_{K1}$ = 7.82, 7.00 and 4.17 for $Pb(OH)^+$, $Cu(OH)^+$, $Cd(OH)^+$, and the first stability constant of the associated metal nitrates ($Me^{2+} + NO_3^- \leftrightarrow Me(NO_3)^+$; $\log_{K1}$ = 1.18, 0.96, and 0.40 for $Pb(NO_3)^+$, $Cu(NO_3)^+$, and $Cd(NO_3)^+$, respectively [57]. On the other hand, based on the calculated mass transfer coefficients from polymer supported ultrafiltration (PSU) process the coordination affinity of these metals to neat BPEI has been estimated as Cu(II) >> Pb(II) >> Cd(II).[58]

As aforementioned, neat BPEI incorporates a high number of amine groups, which exist in primary, secondary and tertiary forms, and it forms coordination pockets for various metal ions. During cross-linking reaction of BPEI to GO, primary amines are being used as the anchoring groups, and therefore, after the condensation reaction cannot be exploited in the coordination of metal ions. The difference in the affinity of the three metal ions to BPEI and GO-BPEI can be explained by the variations in the nature of the coordination pockets, which possess unlike affinities to metal ions before and after grafting BPEI to GO. In the present case, competitive complexation of metal ions on GO-BPEI was studied by the means of binary and tertiary metal mixtures and adsorption experiments (see Figure S15, ESI†). The affinity order for GO-BPEI agrees very well with first stability constant of the associated metal hydroxide and metal nitrates.

We have studied the influence of Pb(II), Cd(II), Cu(II) adsorption on GO-BPEI in the presence of the background electrolyte ($NaNO_3$) at different concentrations. The effect of background electrolyte on the sorption of heavy metal ions at three different concentrations, i.e. 0.01, 0.05 and 0.1 mol L^{-1} was investigated at the best performing experimental conditions, namely at the pH = 5. As shown in Figure S16, ESI† adsorption of Pb(II), Cd(II), Cu(II) ions on GO-BPEI is not affected by the presence of $NaNO_3$ Additional adsorption experiment were carried out by using tap water, and the results were compared with those obtained for MiliQ water, revealing that the presence of mono and divalent metal ions like Na(I), K(I), Ca(II), Mg(II) does not influence the q_{max} values of heavy metal uptake (see Fig. S17 in ESI†). Finally, the regeneration of the GO-BPEI composite is demonstrated by performing adsorption cycles. To this end, the composite is repeatedly immersed in the aqueous solutions of heavy metal ions and treated with 0.1 M solution of either ethylenediaminetetraacetic acid (EDTA) or nitric acid (see *Reusability of GO-BPEI composite* in ESI†). It revealed that HNO_3 treatment allows

reaching high regeneration efficiency compared to EDTA. The overall decrease in adsorption capacity after ten cycles is found smaller than in the EDTA treated foam, and it amounts to 45% for Cu(II), 20% for Pb(II) and 33% for Cd(II) ions.

Conclusions

In this work, we have described a supramolecular, facile and modular approach to the fabrication of 3D GO-based adsorbent, i.e. GO-BPEI, formed through condensation between GO and BPEI. GO-based 3D foams are particularly appealing for the efficient removal of heavy metal ions from water since they expose numerous oxygen- and nitrogen-containing functional groups, which can interact at the supramolecular level with the metal ions. The GO-BPEI foam generates supramolecular pockets that are particularly suitable for sequestering specific metal ions. This is evidenced by remarkably high maximum adsorption capacities towards heavy metal ions at pH 5: 1096, 2051, and 3390 mg g^{-1} for Cu(II), Cd(II) and Pb(II), respectively. These values are much larger than those of any known sorbents including GO and GO-based adsorbents. The non-covalent, thus reversible nature of interactions between the GO based foam and the metal ions is key in order to re-generate the foam. We have showed that the adsorbed metal ions can be removed with treatments of either EDTA or nitric acid. The presented results demonstrate the chemical tailoring of GO-based composites enables to develop highly performing adsorbent for efficient wastewater purification and offer a new avenue towards the effective removal of heavy metal pollutants at large scale. Thermodynamic calculations showed that the adsorption process of heavy metal ions had exothermic and spontaneous nature.

Conflicts of interest

There are no conflicts of interest to declare.

Acknowledgements

This work was supported by the European Commission through the Graphene Flagship Core 1 project (GA-696656) and the Polish National Science Centre (Grant no. 2015/18/E/ST5/00188 and Grant no. 2016/21/B/ST5/00175). We also are thankful for the support of the Agence Nationale de la Recherche through the LabEx project Chemistry of Complex Systems (ANR-10-LABX-0026_CSC), the International Center for Frontier Research in Chemistry (icFRC). D.P. and S.W. acknowledges the support from the Embassy of France in Poland in the form of a scholarship at the Institut de Science et d'Ingénierie Supramoléculaires, University of Strasbourg.

1. J. O. Lundberg, E. Weitzberg, J. A. Cole and N. Benjamin, *Nat. Rev. Microbiol.*, 2004, **2**, 593.
2. E. Diamanti-Kandarakis, J.-P. Bourguignon, L. C. Giudice, R. Hauser, G. S. Prins, A. M. Soto, R. T. Zoeller and A. C. Gore, *Endocr. Rev.*, 2009, **30**, 293-342.
3. R. P. Schwarzenbach, B. I. Escher, K. Fenner, T. B. Hofstetter, C. A. Johnson, U. von Gunten and B. Wehrli, *Science*, 2006, **313**, 1072-1077.
4. J. Lubchenco, *Science*, 1998, **279**, 491-497.
5. I. Ali, *Chem. Rev.*, 2012, **112**, 5073-5091.
6. D. Vilela, J. Parmar, Y. Zeng, Y. Zhao and S. Sánchez, *Nano Lett.*, 2016, **16**, 2860-2866.
7. I. Ali and V. K. Gupta, *Nat. Protocols*, 2007, **1**, 2661-2667.
8. B. Li, Y. Zhang, D. Ma, Z. Shi and S. Ma, *Nat. Commun.*, 2014, **5**, 5537.

9. F. Perreault, A. Fonseca de Faria and M. Elimelech, *Chem. Soc. Rev.*, 2015, **44**, 5861-5896.
10. E. A. Müller, L. F. Rull, L. F. Vega and K. E. Gubbins, *J. Phys. Chem.*, 1996, **100**, 1189-1196.
11. A. Dąbrowski, *Adv. Colloid Interface Sci.*, 2001, **93**, 135-224.
12. G. Crini, *Bioresour. Technol.*, 2006, **97**, 1061-1085.
13. E. S. Cho, J. Kim, B. Tejerina, T. M. Hermans, H. Jiang, H. Nakanishi, M. Yu, A. Z. Patashinski, S. C. Glotzer, F. Stellacci and B. A. Grzybowski, *Nat. Mater.*, 2012, **11**, 978-985.
14. Y. Peng, H. Huang, Y. Zhang, C. Kang, S. Chen, L. Song, D. Liu and C. Zhong, *Nat. Commun.*, 2018, **9**.
15. D. Tasis, N. Tagmatarchis, A. Bianco and M. Prato, *Chem. Rev.*, 2006, **106**, 1105-1136.
16. E. Vázquez and M. Prato, *ACS Nano*, 2009, **3**, 3819-3824.
17. X. Huang, Z. Yin, S. Wu, X. Qi, Q. He, Q. Zhang, Q. Yan, F. Boey and H. Zhang, *Small*, 2011, **7**, 1876-1902.
18. Q. Ma, Y. Yu, M. Sindoro, A. G. Fane, R. Wang and H. Zhang, *Adv. Mater.*, 2017, **29**, 1605361-n/a.
19. S. Eigler and A. Hirsch, *Angew. Chem. Int. Ed.*, 2014, **53**, 7720-7738.
20. D. Chen, H. Feng and J. Li, *Chem. Rev.*, 2012, **112**, 6027-6053.
21. S. Park and R. S. Ruoff, *Nat. Nanotechnol.*, 2009, **4**, 217.
22. K. Parvez, S. Yang, Y. Hernandez, A. Winter, A. Turchanin, X. Feng and K. Müllen, *ACS Nano*, 2012, **6**, 9541-9550.
23. R. K. Joshi, S. Alwarappan, M. Yoshimura, V. Sahajwalla and Y. Nishina, *Appl. Mater. Today*, 2015, **1**, 1-12.
24. D. Cohen-Tanugi and J. C. Grossman, *Nano Lett.*, 2012, **12**, 3602-3608.
25. V. Chandra, J. Park, Y. Chun, J. W. Lee, I. C. Hwang and K. S. Kim, *ACS Nano*, 2010, **4**, 3979-3986.
26. P. Sun, M. Zhu, K. Wang, M. Zhong, J. Wei, D. Wu, Z. Xu and H. Zhu, *ACS Nano*, 2013, **7**, 428-437.
27. R. Liu, T. Gong, K. Zhang and C. Lee, *Sci. Rep.*, 2017, **7**, 9761.
28. P.-X. Hou, H. Orikasa, T. Yamazaki, K. Matsuoka, A. Tomita, N. Setoyama, Y. Fukushima and T. Kyotani, *Chem. Mater.*, 2005, **17**, 5187-5193.
29. D. Chen, H. Zhu, S. Yang, N. Li, Q. Xu, H. Li, J. He and J. Lu, *Adv. Mater.*, 2016, **28**, 10443-10458.
30. İ. Duru, D. Ege and A. R. Kamali, *J. Mat. Sci.*, 2016, **51**, 6097-6116.
31. R. Sitko, E. Turek, B. Zawisza, E. Malicka, E. Talik, J. Heimann, A. Gagor, B. Feist and R. Wrzalik, *Dalton Trans.*, 2013, **42**, 5682-5689.
32. G. Zhao, J. Li, X. Ren, C. Chen and X. Wang, *Environ. Sci. Technol.*, 2011, **45**, 10454-10462.
33. L. Xu and J. Wang, *Crit. Rev. Environ. Sci. Technol.*, 2017, **47**, 1042-1105.
34. W. Peng, H. Li, Y. Liu and S. Song, *J. Mol. Liq.*, 2017, **230**, 496-504.
35. W.-S. Hung, C.-H. Tsou, M. De Guzman, Q.-F. An, Y.-L. Liu, Y.-M. Zhang, C.-C. Hu, K.-R. Lee and J.-Y. Lai, *Chem. Mater.*, 2014, **26**, 2983-2990.
36. Z. Y. Sui, Y. Cui, J. H. Zhu and B. H. Han, *ACS Appl. Mater. Interfaces*, 2013, **5**, 9172-9179.
37. X. Zhang, A. Ciesielski, F. Richard, P. Chen, E. A. Prasetyanto, L. De Cola and P. Samorì, *Small*, 2016, **12**, 1044-1052.

38. Z. Yuan, H. Tai, Z. Ye, C. Liu, G. Xie, X. Du and Y. Jiang, *Sens. Actuator B-Chem.*, 2016, **234**, 145-154.
39. Y. Huang, D. Wu, A. Dianat, M. Bobeth, T. Huang, Y. Mai, F. Zhang, G. Cuniberti and X. Feng, *J. Mater. Chem. A*, 2017, **5**, 1588-1594.
40. B. Chen, M. Liu, L. Zhang, J. Huang, J. Yao and Z. Zhang, *J. Mater. Chem.*, 2011, **21**, 7736-7741.
41. S. Kumar, S. Raj, K. Sarkar and K. Chatterjee, *Nanoscale*, 2016, **8**, 6820-6836.
42. L. Zhang, Z. Lu, Q. Zhao, J. Huang, H. Shen and Z. Zhang, *Small*, 2011, **7**, 460-464.
43. Y. Liu, Y. Fan, Y. Yuan, Y. Chen, F. Cheng and S.-C. Jiang, *J. Mater. Chem.*, 2012, **22**, 21173-21182.
44. Y. Yan, Q. An, Z. Xiao, W. Zheng and S. Zhai, *Chem. Eng. J.*, 2017, **313**, 475-486.
45. J. Meng, J. Cao, R. Xu, Z. Wang and R. Sun, *J. Mater. Chem. A*, 2016, **4**, 11656-11665.
46. J. Jia, A. H. Wu and S. J. Luan, *Colloids Surf., A*, 2014, **449**, 1-7.
47. A. H. Wu, J. Jia and S. J. Luan, *Colloids Surf. A*, 2011, **384**, 180-185.
48. Y. Xu, H. Bai, G. Lu, C. Li and G. Shi, *J. Am. Chem. Soc.*, 2008, **130**, 5856-5857.
49. S. Chen, J. Zhu, X. Wu, Q. Han and X. Wang, *ACS Nano*, 2010, **4**, 2822-2830.
50. M. Herrera-Alonso, A. A. Abdala, M. J. McAllister, I. A. Aksay and R. K. Prud'homme, *Langmuir*, 2007, **23**, 10644-10649.
51. O. C. Compton, D. A. Dikin, K. W. Putz, L. C. Brinson and S. T. Nguyen, *Adv. Mater.*, 2010, **22**, 892-896.
52. C. Y. Su, Y. P. Xu, W. J. Zhang, J. W. Zhao, A. P. Liu, X. H. Tang, C. H. Tsai, Y. Z. Huang and L. J. Li, *Acs Nano*, 2010, **4**, 5285-5292.
53. X. Zhang, Y. Huang, Y. Wang, Y. Ma, Z. Liu and Y. Chen, *Carbon*, 2009, **47**, 334-337.
54. Z. Zhang, X. Ma, D. Wang, C. Song and Y. Wang, *AIChE J.*, 2012, **58**, 2495-2502.
55. C. Y. Yin, M. K. Aroua and W. M. A. W. Daud, *Water Sci. Technol.*, 2007, **56**, 95-101.
56. C. Y. Yin, M. K. Aroua and W. M. A. W. Daud, *Water Air Soil Pollut.*, 2008, **192**, 337-348.
57. J. A. Dean, *McGraw-Hill, New York,*, 1999.
58. P. Canizares, A. Perez and R. Camarillo, *Desalination*, 2002, **144**, 279-285.

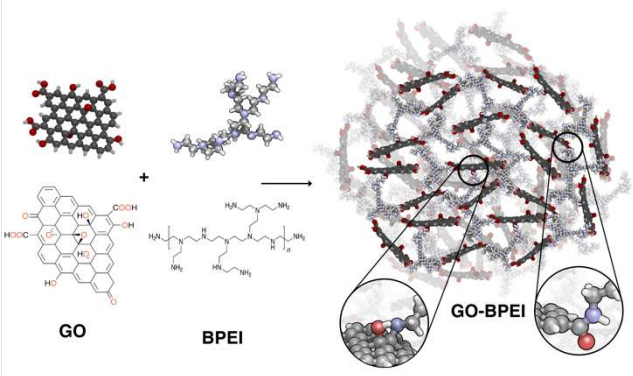

Fig. 1 Schematic representation of the GO-BPEI synthesis. The GO-BPEI composite is generated through the condensation reaction between graphene oxide (GO) and branched polyethylenimine (BPEI).

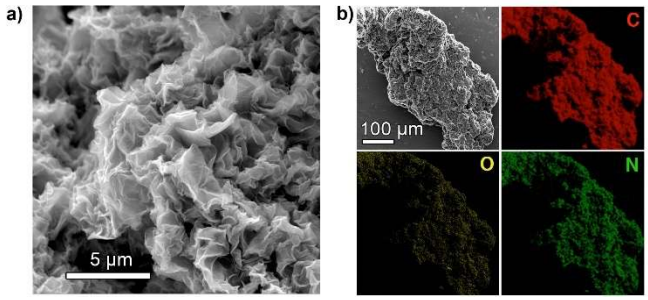

Fig. 2 Morphological characterization of graphene oxide cross-linked with polyethylenimine (GO-BPEI). (a) Scanning electron microscopy (SEM) image displaying the morphology of GO-BPEI foam, (b) SEM image of GO-BPEI fragmented foam and EDX elemental mapping of carbon (C), oxygen (O) and nitrogen (N).

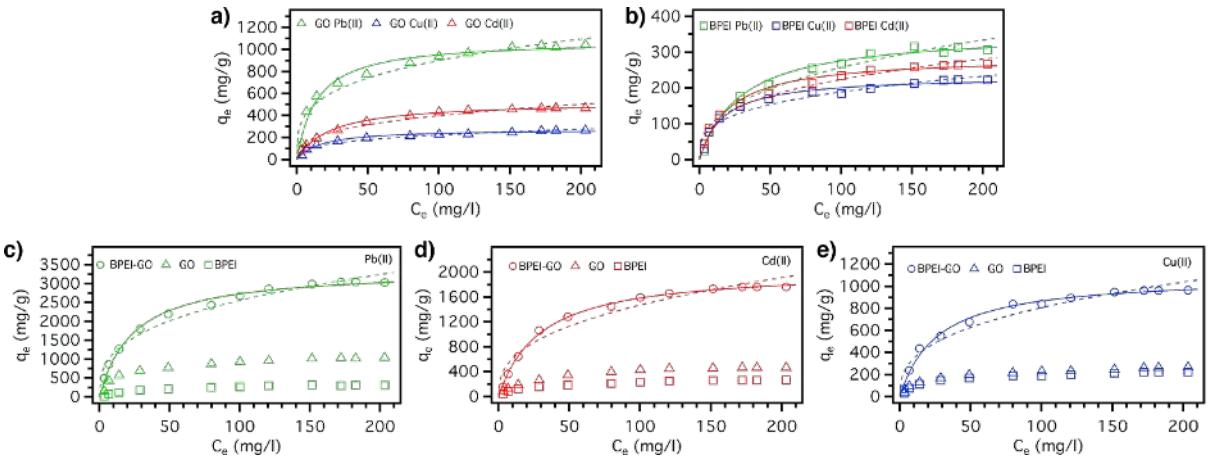

Fig. 3 Uptake of heavy metal ions as a function of Cu(II), Cd(II) and Pb(II) concentration in aqueous solution. Adsorption isotherms on control samples: (a) unfunctionalized graphene oxide GO, (b) neat branched polyethylenimine (BPEI), and foam generated upon cross-linking GO with polyethylenimine (GO-BPEI) (c,d,e). The uptake experiments are carried at pH = 5 ($C_{GO,BPEI,GO\text{-}BPEI}$ = 0.05 g L-1, T = 25 °C, stirring speed = 200 rpm, t = 12 h). The experimental adsorption data are fitted with Langmuir (solid lines) and Freundlich (dashed lines) models.

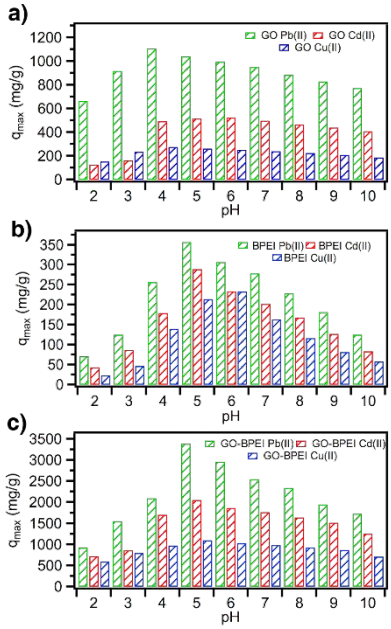

Fig. 4. The influence of pH on the maximum adsorption capacity and GO-BPEI regeneration. Variations of the pH of Pb(II), Cd(II), Cu(II) aqueous solutions are investigated and are found to strongly affect the maximum adsorption capacity on (a) GO, (b) BPEI, and (c) GO-BPEI.